

# Simulation of Vapor–Liquid Phase Equilibria of Primary Alcohols and Alcohol–Alkane Mixtures

Rajesh Khare,<sup>†,§</sup> Amadeu K. Sum,<sup>\*,‡</sup> Shyamal K. Nath,<sup>†,||</sup> and Juan J. de Pablo<sup>‡</sup>

Accelrys Inc., 9685 Scranton Road, San Diego, California 92121 and Department of Chemical & Biological Engineering, University of Wisconsin-Madison, Madison, Wisconsin 53706

Received: April 28, 2004

The NERD force field (Nath, S. K.; Escobedo, F. A.; de Pablo, J. J. *J. Chem. Phys.* **1998**, *108*, 9905) is extended to include parameters for modeling primary alcohols. Gibbs ensemble simulations are performed for the pure component vapor–liquid equilibria of the homologous series of alcohols from ethanol to 1-octanol. Our results show that the simulated values of the saturated liquid densities and critical constants of the alcohols are within a few percent of the corresponding experimental data. In addition, the simulated pressure composition diagram for a binary mixture of heptane and 1-pentanol also shows satisfactory agreement with the experimental data.

## Introduction

Alcohols constitute an important class of compounds because of their amphiphilic character. They are widely used as solvents in industrial processes, and their molecular structure is of theoretical interest because of their tendency to form hydrogen-bonded networks.

Several studies in the literature have focused on modeling the structural, thermophysical, and dynamic properties of methanol at the molecular level.<sup>1–3</sup> Structural and thermophysical properties of short-chain alcohols have also been studied by molecular simulation.<sup>1,4</sup> Jorgensen<sup>4</sup> extended the OPLS set of potential parameters to study structural and thermodynamic properties of short-chain alcohols. In that work, results for the liquid density, heat of vaporization, heat capacities, and isothermal compressibilities were in excellent agreement with experimental data for several alcohols (methanol, ethanol, 1-propanol, 2-propanol, and 2-methyl-2-propanol).

Large amounts of experimental data are also available for pure component vapor–liquid equilibria and phase equilibria for mixtures of alcohols and alkanes.<sup>5–9</sup> In general, alcohols and alkanes form highly nonideal mixtures that exhibit azeotropes.

With the advent in recent years of newer simulation techniques,<sup>10</sup> phase equilibria calculations for a large number of compounds have become possible, including hydrocarbons and alcohols. Gibbs ensemble simulations by van Leeuwen and Smit<sup>11</sup> showed that previous molecular models for methanol<sup>2,4</sup> were unable to satisfactorily describe its phase behavior along the phase boundary. This observation prompted those authors to develop a new molecular model for methanol that could accurately predict the phase coexistence properties for methanol. In a later study by van Leeuwen,<sup>12</sup> Gibbs ensemble simulations on the homologous series of alcohols indicated that the force field developed by Jorgensen<sup>4</sup> was satisfactory in predicting the

vapor–liquid equilibria for small alcohols (up to propanol), but the results showed significant deviations from experimental values for hexanol. It was shown that a modified set of force field parameters yielded reasonable agreement with experimental vapor–liquid equilibria for both 1-hexanol and 3-hexanol.

Recently, Chen et al.<sup>13</sup> have extended the TraPPE-UA force field for generic alcohols. In that work, Gibbs ensemble simulations were performed to show that the predicted values of saturated liquid densities and the critical temperature and density for primary, secondary, and tertiary alcohols were within a few percent of the corresponding experimental data. In addition, phase equilibrium calculations in the grand canonical ensemble for mixtures of *n*-hexane/methanol and *n*-hexane/ethanol overpredicted the equilibrium pressures over the entire composition range; however, the azeotropic composition determined by simulation was in good agreement with experimental data. A binary mixture of methanol and *n*-hexane was also studied by Potoff et al.<sup>14</sup> using grand canonical histogram reweighting Monte Carlo simulations, with a nontraditional exponential-6 potential; their predicted pressure composition diagram showed satisfactory agreement with experiments at two different temperatures.

Several years ago, Nath et al.<sup>15–17</sup> developed the NERD force field for vapor–liquid equilibrium predictions of alkanes using Gibbs ensemble simulations. Since then, the force field has been extended to include branched alkanes,<sup>16</sup>  $\alpha$ -olefins,<sup>17</sup> and their mixtures.<sup>18</sup> Recently, additional parameters were added to the NERD force field for molecules containing polar groups, including carbonyl and ester groups,<sup>19</sup> hydrogen sulfide,<sup>20</sup> alkyl sulfides and thiols,<sup>21</sup> and dimethyl ether.<sup>22</sup> This paper describes an extension of the NERD force field to alcohols, in particular, the homologous series of primary alcohols from ethanol to 1-octanol. As previously found in the COMPASS all-atom force field,<sup>23</sup> special parameters are required for representing methanol, the shortest member of the alkanol series (this approach differs from the philosophy of the TraPPE force field where a single set of parameters is used for all primary alcohols including methanol<sup>13</sup>). Results for pure component and mixture vapor–liquid equilibria of methanol will be presented in a separate study.

\* To whom correspondence should be addressed. E-mail: sum@che.wisc.edu.

<sup>†</sup> Accelrys.

<sup>‡</sup> University of Wisconsin-Madison.

<sup>§</sup> Present e-mail address: rkhare@mail.sdsu.edu.

<sup>||</sup> Present address: Department of Materials Engineering, New Mexico Tech, Socorro, NM 87801.

The force field parameters for primary alcohols proposed here are consistent with the current parameters of functional groups already available in the NERD force field. The paper is organized as follows: we begin by providing details of the molecular model, including the procedure used for developing the force field parameters for alcohols. Details of the simulation methodology are presented next, followed by results for the pure component vapor–liquid equilibria of alcohols from ethanol to 1-octanol and for the binary mixture *n*-heptane/1-pentanol. We conclude the paper with a summary of the results.

## Method

**Molecular Model.** In the original NERD model,<sup>15–17</sup> the united atom approach was used for representing the CH, CH<sub>2</sub>, and CH<sub>3</sub> groups of alkanes and alkenes (chosen for matters of computational efficiency of the simulations). For molecules containing polar groups (hydroxyl group in this case), the partial charge on the hydrogen atom plays a crucial role in the behavior of the molecule. Given these considerations, the hydrogen atom for the hydroxyl group on the alcohols is explicitly considered in our model, whereas all the other hydrogen atoms in the molecule are treated using a united atom approach, that is, by collapsing them onto the carbon atoms (methyl and methylene) to which they are attached, thus maintaining the NERD model description. A similar approach has been previously employed in the literature for the extension of united atom force fields to molecules containing polar groups;<sup>4,13</sup> this approach has also been employed in the NERD development work for the treatment of other polar groups such as those found in thiols.<sup>21</sup>

Intramolecular interactions for the model system are treated using the functional form of the NERD potential; specifically, harmonic potentials for the bond-stretching and bond-bending interactions and a Fourier-cosine series for the torsion potential. More details on the intramolecular potential can be found in previous publications.<sup>16,17</sup>

Nonbonded interactions are considered for atoms that belong to different molecules or for atoms that are separated by more than three atoms on the same molecule (i.e., atoms that are not interacting by any of the intramolecular potentials). Nonbonded interactions are modeled using the Lennard-Jones 12–6 potential along with the Lorentz–Berthelot combining rules for the interaction parameters between unlike pairs.<sup>24</sup> When a hydrogen atom is modeled explicitly in the extensions of united atom models, a common practice in the literature has been to place only a point charge on this atom and ignore its Lennard-Jones interactions. However, in the previous extension of the NERD force field to hydrogen sulfide,<sup>20</sup> Lennard-Jones interactions were considered for all of the atoms in the system including the explicit hydrogen atoms; the same approach is adopted in this work.

**Force Field Development.** The NERD force field has been extensively parametrized for alkanes and alkenes. For the primary alcohol molecules considered in this work, the only new functional group is the hydroxyl group. The parameters for representing the hydroxyl group were developed in this work, and existent alkane parameters were used for the alkyl part of the alcohols. The parametrization proceeded in two stages. First, intramolecular potential energies and atomic partial charges were determined using quantum chemical calculations. Parameters for the Lennard-Jones interactions were subsequently determined using Gibbs ensemble phase equilibria simulations.

The first step in our ab initio quantum chemical calculations was to establish the equilibrium geometry of the molecule. In this work, parameters were developed by considering 1-pentanol

**TABLE 1: Extended NERD Force Field for Alcohols**

bond stretching	$K_r$ , kJ/(mol·Å <sup>2</sup> )	$r_{eq}$ , Å	
CH <sub>3</sub> –CH <sub>2</sub>	2800	1.540	
CH <sub>2</sub> –O	3300	1.428	
O–H	5200	0.961	
bonds bending	$K_\theta$ , kJ/(mol·rad <sup>2</sup> )	$\theta_{eq}$ , degree	
CH <sub>3</sub> –CH <sub>2</sub> –CH <sub>2</sub>	760	114.0	
CH <sub>2</sub> –CH <sub>2</sub> –O	1000	108.0	
CH <sub>2</sub> –O–H	460	107.5	
torsion potential			
CH <sub>3</sub> –CH <sub>2</sub> –CH <sub>2</sub> –CH <sub>2</sub>	$V_0 = 0.000$ , $V_1 = 2.952$ , $V_2 = -0.567$ , $V_3 = 6.579$ kJ/mol		
CH <sub>2</sub> –CH <sub>2</sub> –CH <sub>2</sub> –O	$V_0 = 1.929$ , $V_1 = 2.963$ , $V_2 = -3.926$ , $V_3 = 9.311$ kJ/mol		
CH <sub>2</sub> –CH <sub>2</sub> –O–H	$V_0 = 0.000$ , $V_1 = 2.987$ , $V_2 = 0.491$ , $V_3 = 1.836$ kJ/mol		
Lennard-Jones parameters	$\epsilon$ , kJ/mol	$\sigma$ , Å	$q$ , au
H	0.0324	0.98	0.420
O	0.8979	2.98	−0.710
CH <sub>2</sub> <sup>b</sup>	0.3808	3.93	0.290
CH <sub>2</sub>	0.3808	3.93	0.000
CH <sub>3</sub>	0.8647	3.91	0.000

<sup>a</sup> Intramolecular potential parameters and partial charges calculated from quantum chemical calculations. Lennard-Jones parameters optimized to fit vapor–liquid equilibrium data. <sup>b</sup> Bonded to hydroxyl group.

as a representative molecule for the alcohols. A geometry optimization was performed with MP2/6-311++G(*d,p*) using the Gaussian suite of programs.<sup>25</sup> The next task was to determine the intramolecular potentials corresponding to bond stretching, bond angle bending, and torsions. It was assumed, to a first approximation, that all these three interactions are uncoupled and they can be calculated independently of each other. In such a case, perturbation around the equilibrium value of the bond length or angle can be imposed on the geometry of the molecule, and the potential energy of the resulting structure can be determined as a function of the degree of perturbation. For the bond-stretching potential, each bond (excluding those between the methyl/methylene hydrogens) was contracted and expanded by 0.12 Å from its equilibrium bond length in intervals of 0.02 Å. For the bond angle bending potential, each angle (also excluding those involving methyl/methylene hydrogens) was varied  $\pm 12$  degrees from its equilibrium value in intervals of 2 degrees. Finally, for the torsion potential, any given torsion angle was incremented in steps of 15 degrees up to a total change of 180 degrees from the equilibrium conformation. Following these structural changes, a single-point energy calculation with MP2/6-311++G(*df,pd*) was performed for every perturbed geometry to construct the potentials. The parameters (force constants and Fourier coefficients) obtained by fitting the energy surface to the NERD functional form are shown in Table 1.

Partial charges on the atoms were determined from a fit of the electrostatic potential energy surface using Gaussian with MP2/6-311++G(*df,pd*). The resulting values of the partial charges are also listed in Table 1. Given the united atom nature of the model (and to be consistent with the previously used parameters for alkanes), partial charges are only considered for three atoms (hydroxyl group atoms and united atom CH<sub>2</sub> adjacent to the hydroxyl group) in our model alcohols. The adjusted partial charges yield a dipole moment of 2.32 D for 1-pentanol, which is higher than the experimental value of 1.69 D for this molecule.<sup>26</sup> The actual charges obtained from the calculations of the electrostatic potential energy surface yield a dipole moment of 1.73 D; however, because of the restrictions

imposed by the model and the requirement of electroneutrality of the molecule, the final set of adjusted partial charges yield a higher dipole moment. This discrepancy in the values of the dipole moment is not unusual; we focus on condensed-phase properties and it is known that the dipole moment values for molecules in a liquid phase are usually higher than those reported for the same molecules in a vapor phase (e.g., for SPC water, the dipole moment is 2.27 D,<sup>27</sup> whereas the dipole of water in the vapor phase is 1.8 D<sup>26</sup>).

Once atomic partial charges and parameters for the intramolecular potentials were determined, these were held fixed and nonbonded interaction parameters for the Lennard-Jones potential were adjusted to minimize the error on the vapor–liquid equilibria for pentanol between that predicted in simulation and experimental data. As previously mentioned, the CH<sub>3</sub> and CH<sub>2</sub> united atoms of the alkyl chain (including the CH<sub>2</sub> group adjacent to the hydroxyl group) retained the Lennard-Jones parameters used in the NERD force field for alkanes. Of the remaining two atoms, namely, the oxygen and hydrogen atoms of the OH group, Lennard-Jones parameters for the hydrogen atom were taken from earlier work.<sup>20</sup> Only parameters for the oxygen atom were optimized. Lennard-Jones parameters for oxygen were adjusted to obtain the best agreement with experimental saturated liquid densities and critical temperature and density using Gibbs ensemble simulations. The complete set of force field parameters for 1-pentanol is listed in Table 1.

**Phase Equilibria Simulations.** Pure component and mixture vapor–liquid equilibria were obtained using *NVT* and *NPT* Gibbs ensemble Monte Carlo simulations (which were carried out using the equilibria phase equilibrium simulation program<sup>28</sup>), respectively. Simulations for the pure component vapor–liquid equilibrium contained at least 160 molecules, and both equilibration and production stages for the high-temperature runs consisted of at least  $5 \times 10^6$  moves. Longer simulations were required for the low temperatures and all of the mixture systems. A cutoff distance of 10 Å was used for the nonbonded interactions, with long-range corrections applied beyond this distance for the van der Waals interactions. Electrostatic interactions between polar groups play an important role in determining the thermodynamic behavior of molecules containing these groups and are significant over a much longer length scale (decay as  $r^{-1}$ ) than the van der Waals interactions.

Several approaches are often used for treating the long-range part of the electrostatic interactions; these include cell multipole methods,<sup>29</sup> Ewald summations,<sup>24</sup> and the use of charge-group based cutoffs.<sup>30,31</sup> The charge-group based cutoff approach is adopted in this work because it is more efficient and comparable in accuracy to Ewald summation methods;<sup>23,31</sup> A charge group is a net neutral collection of atoms that are in close spatial proximity, and in practice, they consist of net neutral segments of atoms that are covalently bonded. Each charge group also has a designated switching atom that is ideally an atom close to the geometrical centroid of the charge group. For alcohols, the only significant charge group consists of the hydroxyl oxygen atom (switching atom), the hydroxyl hydrogen atom, and the CH<sub>2</sub> unit adjacent to the hydroxyl group. (In addition, each of the remaining CH<sub>2</sub> and CH<sub>3</sub> units could also comprise individual charge groups, but these do not have any partial charge in the current force field.) During simulations, charge-group based cutoffs are applied according to the distance between the switching atoms of the charge groups; if the distance between the switching atoms of two charge groups is less than the specified cutoff distance, electrostatic interactions between all pairs of atoms belonging to the two charge groups are

calculated. On the other hand, if the distance between the switching atoms is greater than the cutoff distance, electrostatic interactions between all pairs of atoms belonging to the two charge groups are neglected. Such an approach only neglects dipole–dipole interactions at the cutoff distance, unlike cutoffs on an atom-by-atom basis, where charge–charge interactions can be unaccounted. Selected simulations were also performed with Ewald summations to verify the accuracy of our results.

Because of large fluctuations near the critical point, it is not possible to explicitly determine its location. An approach often employed to determine the critical point requires several simulations at subcritical temperatures and then extrapolation of these data using the Ising scaling method to obtain an estimate of the critical point.<sup>15,32,33</sup> For alkanes, a typical value of 0.32 for the Ising scaling exponent yields a good description of vapor–liquid equilibrium data.<sup>15,32,33</sup> However, this is not the case for molecules containing polar groups, such as for alcohols. In such a case, an “effective” Ising scaling exponent is obtained from a fit of available experimental data for these systems. Here, we have used the exponents reported in the literature<sup>34</sup> for the systems under consideration.

**Vapor-Pressure Calculations.** In addition to the Gibbs ensemble simulations for determination of vapor–liquid equilibria, we also performed constant *NPT* Monte Carlo simulations of the vapor phase to determine the vapor pressure as a function of temperature. The vapor phase in these simulations contained 10 molecules. At a given temperature, the vapor pressure was the pressure, which yielded the same density as the vapor density at the vapor–liquid coexistence as determined by Gibbs ensemble simulations. In practice, *NPT* Monte Carlo simulations were performed at five different pressures at any given temperature. These simulations are fast, and a linear fit of the pressure–density data was used to determine the vapor pressure corresponding to the equilibrium vapor density. We elected to use this method to determine the vapor pressure because the pressure was not directly calculated in the Gibbs ensemble simulations.

## Results

**Pure Component Vapor–Liquid Equilibria.** The phase diagram of 1-pentanol obtained in this work is shown in Figure 1. The solid line curve in Figure 1 represents the Ising scaling fit to the simulated data using a scaling exponent of 0.29. The fit proposed here is able to describe the data with high accuracy.

The results for 1-pentanol provide a complete set of parameters required to predict vapor–liquid equilibria for the other primary alcohols, ranging from ethanol to 1-octanol. Figure 2 shows predicted vapor–liquid equilibrium for ethanol, 1-propanol, and 1-butanol, while Figure 3 plots the phase equilibrium diagrams for 1-hexanol and 1-octanol (results for 1-heptanol are of similar quality and have been omitted for clarity).

In previous work, Chen et al.<sup>13</sup> found that the predicted values of saturated liquid densities using their TraPPE force field parameters for alcohols were within 1% of the experimental values. Furthermore, they found that on average, their force field overestimated the critical densities by about 3% and underestimated the critical temperatures by about 1.5%. In comparison, on an average, the saturated liquid densities for all the alcohols considered here are also within 1% of the corresponding experimental values at all temperatures investigated. Critical constants obtained using the Ising scaling method are summarized in Table 2. On average, predicted critical temperatures and densities deviate about 1.6 and 2.2%, respectively, from the corresponding experimental values (in terms of absolute

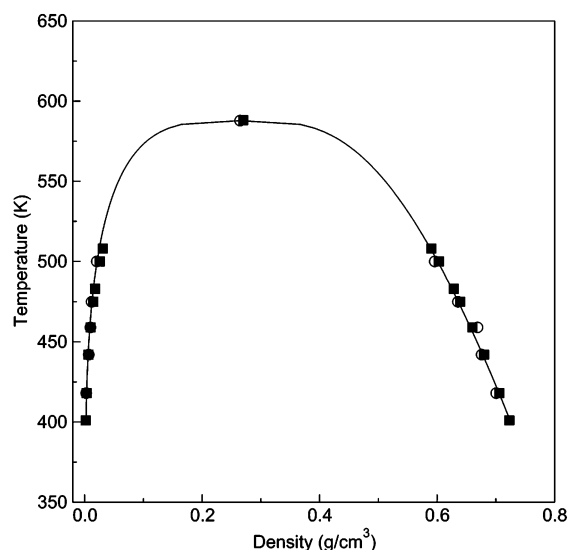


**Figure 1.** Vapor–liquid equilibrium diagram for 1-pentanol. Filled squares and open circles represent experimental data<sup>6</sup> and predicted values from simulations, respectively. Line represents an Ising scaling fit to the predicted data using an Ising scaling exponent of 0.29.

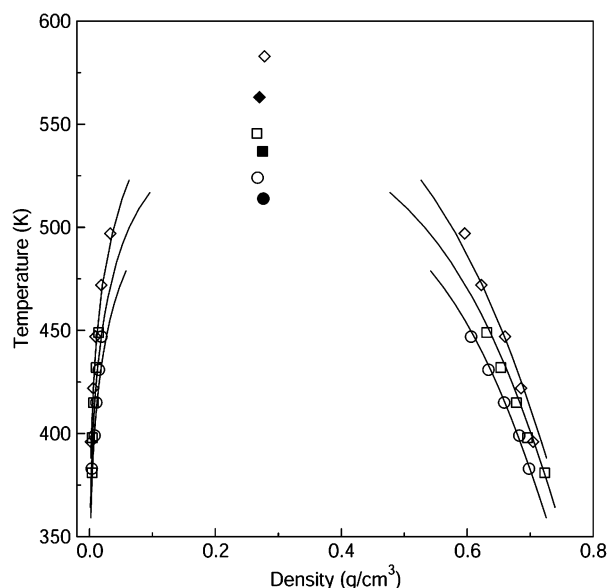


**Figure 2.** Vapor–liquid equilibrium diagrams for ethanol, 1-propanol, and 1-butanol. Symbols correspond to predicted values from simulations: circles, ethanol; squares, 1-propanol; diamonds, 1-butanol. Lines correspond to experimental data.<sup>6</sup> Solid symbols represent experimental critical points.

numbers, these deviations correspond to about 10 K for the critical temperature and 0.006 g/cm<sup>3</sup> for the critical density). The critical properties were predicted using the rather ad hoc approach based on the Ising scaling method with a fitted exponent (see earlier text). Furthermore, we have found that critical properties determined in this way have a large dependence on the simulation results at the highest simulated temperature. Any variation in the results at the highest simulated temperature is amplified by such a fitting procedure.

As pointed out earlier, for the purposes of achieving a substantial computational speed-up, the charge-group based cutoff method was used to account for long-range electrostatic interactions. Figure 4 presents a comparison of the results obtained using the charge-group based cutoff and the Ewald summation methods for the densities of the saturated liquid phase of pentanol and octanol at selected temperatures. The

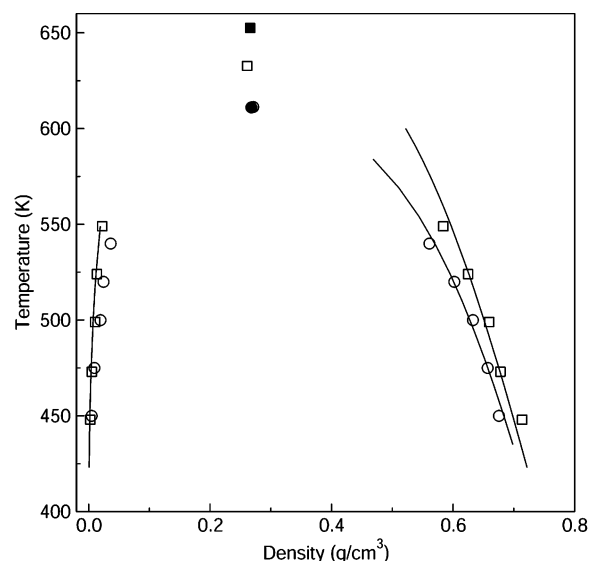


**Figure 3.** Vapor–liquid equilibrium diagrams for 1-hexanol and 1-octanol. Symbols correspond to predicted values from simulations: circles, 1-hexanol; squares, 1-octanol. Lines correspond to experimental data.<sup>6</sup> Solid symbols represent experimental critical points.

**TABLE 2: Simulated and Experimental Values<sup>6</sup> of Critical Properties for Primary Alcohols<sup>a</sup>**

molecule	critical temperature (K)		critical density (g/cm <sup>3</sup> )	
	simulated	experimental	simulated	experimental
ethanol	524.1	513.9	0.267	0.276
1-propanol	545.5	536.8	0.266	0.275
1-butanol	582.9	563.1	0.278	0.270
1-pentanol	587.8	588.2	0.265	0.270
1-hexanol	611.2	611.0	0.271	0.268
1-heptanol	625.6	633.2	0.264	0.267
1-octanol	632.7	652.5	0.261	0.266

<sup>a</sup> An effective Ising scaling exponent of 0.28 is used for ethanol and 0.29 for all other alcohols.

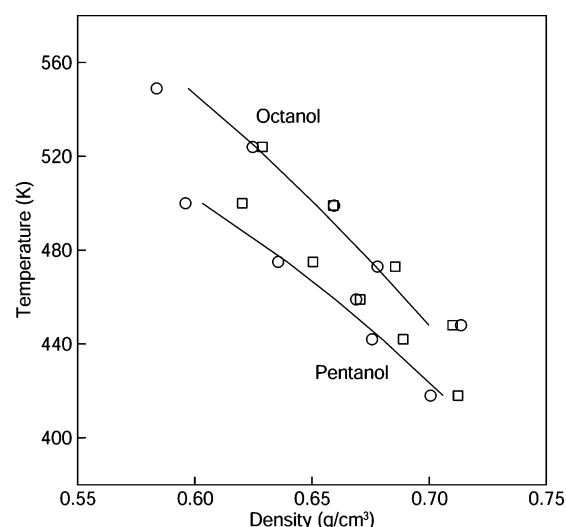


**Figure 4.** Comparison of liquid densities for 1-pentanol and 1-octanol calculated with the charge-group cutoff (circles) and Ewald summation (squares) methods. Solid line corresponds to experimental data.<sup>6</sup>

values reported in the figure were obtained by running constant *NPT* molecular dynamics simulations (using the Discover simulation program<sup>35</sup>) at the vapor pressure of the liquid alcohol (as calculated in this work) at the temperature of interest. The average deviation with Ewald summation for the liquid densities at the selected temperatures is 1.3% from the experimental



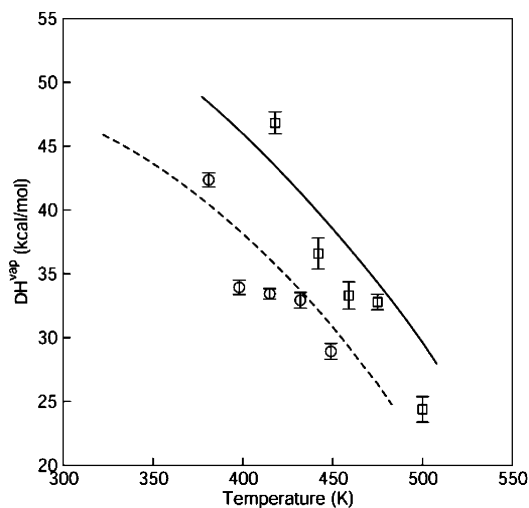


**Figure 5.** Heat of vaporization for propanol (circles) and pentanol (squares) calculated from simulations. Solid lines correspond to experimental data for propanol (dashed) and pentanol (solid).

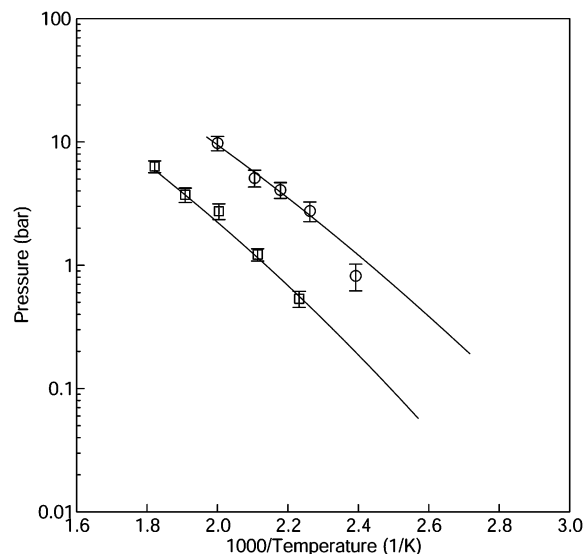


**Figure 6.** Vapor pressure curves for 1-pentanol (circles) and 1-octanol (squares). Lines correspond to experimental data.<sup>6</sup>

values, compared to 1.0% deviation with the charge-group based cutoff method (the average deviation between the Ewald summation and charge-group method results is 1.4%). We consider this level of disagreement between values calculated using various methods to be within acceptable uncertainty (<2%) for the force field.

As an additional test for the force field, the values of heat of vaporization for propanol and pentanol were computed and are plotted as a function of temperature in Figure 5. On an average, the heat of vaporization values are predicted to within 10% of the corresponding experimental values; this level of accuracy appears to be comparable to that obtained using the TraPPE force field.<sup>13</sup>

**Vapor Pressure, Heat Capacity, and Isothermal Compressibility.** In addition to the coexistence densities, vapor (or saturation) pressure is an important quantity for the study of vapor–liquid phase equilibrium. Figure 6 shows a plot of vapor pressure as a function of temperature for 1-pentanol and 1-octanol. As can be seen from the figure, vapor pressures predicted from simulations are in very good agreement with the experimental values for these two alcohols. The one exception is the vapor pressure for pentanol at the lowest

**TABLE 3: Heat Capacity and Isothermal Compressibility for Selected Primary Alcohols**

molecule	heat capacity (J/mol/K)		isothermal comp. (1/atm)	
	calculated	experimental <sup>4</sup>	calculated	experimental <sup>4</sup>
ethanol	116.4	111.96	$7.34 \times 10^{-5}$	$1.16 \times 10^{-4}$
1-propanol	161.3	141.00	$6.65 \times 10^{-5}$	$1.04 \times 10^{-4}$

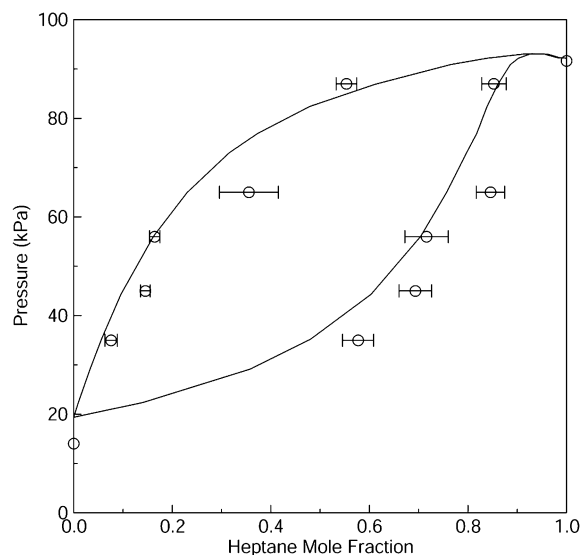


**Figure 7.** Phase diagram ( $P_{xy}$ ) for *n*-heptane/1-pentanol binary mixture at  $T = 368$  K. Open circles are predicted values from simulations and lines correspond to the experimental data.<sup>7</sup> The vapor pressure for pure pentanol shown in the diagram was obtained from an extrapolation of the vapor pressure values calculated at higher temperatures.

temperature considered; we believe this to be a limitation of the force field and the parametrization approach used (after obtaining the intramolecular parameters from the quantum calculations, only the nonbonded parameters of the oxygen atom were fitted to the coexistence densities). From a fit of our data, we calculate normal boiling point values of 418 and 467 K for 1-pentanol and 1-octanol, respectively; these results are in excellent agreement with the reported values of 411 K for 1-pentanol and 468 K for 1-octanol.<sup>36</sup> This level of agreement between the boiling point values predicted using the NERD force field and the experimental values is of similar quality as that obtained using the TraPPE force field for alcohols.<sup>13</sup>

We have also calculated the heat capacity and isothermal compressibility for ethanol and 1-propanol to further assess the ability of the force field to predict physical properties that are not directly related to the phase equilibrium. These quantities were calculated by first running constant  $NPT$  molecular dynamics simulation (using the Discover simulation program<sup>35</sup>) and then applying the appropriate fluctuation formulas. Table 3 presents a comparison of the calculated values of heat capacity ( $C_p$ ) and isothermal compressibility ( $\kappa$ ) with the corresponding experimental data.<sup>4</sup> As can be seen, the values of  $C_p$  and  $\kappa$  show a deviation of less than 15% and 37% from the experimental values, respectively (this agreement is worse than that obtained by Jorgensen<sup>4</sup> using the OPLS force field). Nevertheless, given that the NERD force field was specifically parametrized for predicting phase equilibria, we consider this level of agreement to be reasonable. The results once again highlight the need for developing united atom force fields that can provide an accurate description of a whole range of properties (phase equilibrium, physical and dynamic) simultaneously—a long standing, yet elusive goal.

**Vapor–Liquid Equilibrium for Binary Mixture–Heptane + 1-Pentanol.** Alkanes and alcohols form highly nonideal mixtures and often times the vapor–liquid equilibria of these mixtures are characterized by an azeotrope. One such mixture, heptane/1-pentanol (azeotrope at  $x_{\text{heptane}} = 0.94$ ),<sup>7</sup> was studied in this work with *NPT* Gibbs ensemble simulations and the resulting phase diagram for the mixture at a temperature of 368 K is shown in Figure 7. The Gibbs ensemble simulations for the mixture phase equilibrium proved challenging at times, and very long simulation runs were required in such instances (greater than  $20 \times 10^6$  MC moves). As can be seen from Figure 7, at the selected values of pressures, the predicted composition of the vapor and liquid phases is, in general, in good agreement with the experimental data. The simulations do show a tendency for overprediction of heptane concentration in both phases. The force field parameters used for these calculations were derived solely on the basis of the pure component vapor–liquid equilibria of alkanes and alcohols. The quality of prediction for the mixture diagram could be improved by further modification of the force field parameters for this purpose; however, no such effort was made in this study.

## Summary

Pure component and binary mixture vapor–liquid equilibria of primary alcohols have been studied using Gibbs ensemble simulations. The NERD force field was extended for study of these systems by developing new parameters associated with the hydroxyl group in alcohols. Although NERD was originally developed as a united atom model, the hydrogen atom in the hydroxyl group needs to be explicitly considered in the molecular model for alcohols. Electrostatic interactions in these systems were efficiently handled using the charge-group based cutoff technique. Our results show that predicted coexistence densities, as well as vapor pressures for the pure component vapor–liquid equilibria, are in good agreement with experimental data. Predicted compositions for a vapor–liquid equilibrium of a binary mixture of *n*-heptane/1-pentanol also agree reasonably well with experimental data. One set of parameters is sufficient for a quantitative prediction of phase equilibria of alcohols longer than methanol; however, a separate set of parameters is required to represent methanol.

**Acknowledgment.** The authors thank Dr. David Rigby for his help with the calculations of the heat capacity and isothermal compressibility. R.K. and S.K.N. would also like to thank the Hewlett-Packard Company for providing the computational resources on which most of the calculations presented in this work were performed at Accelrys Inc.

## References and Notes

- Jorgensen, W. L. *J. Am. Chem. Soc.* **1980**, *102*, 543.
- Haughney, M.; Ferrario, M.; McDonald, I. R. *Mol. Phys.* **1986**, *58*, 849.
- Matsumoto, M.; Gubbins, K. E. *J. Chem. Phys.* **1990**, *93*, 1981.
- Jorgensen, W. L. *J. Phys. Chem.* **1986**, *90*, 1276.
- Gmehling, J.; Onken, U.; Arlt, W. *Vapor-Liquid Equilibrium Data Collection*. Vapor-Liquid Equilibrium Data Collection. Frankfurt, Germany: DECHEMA, 1977-onward.
- Smith, B. D.; Srivastava, R. *Thermodynamic Data for Pure Compounds: Part B Halogenated Hydrocarbons and Alcohols*; Elsevier: Amsterdam, 1986.
- Machova, I.; Linek, J.; Wichterle, I. *Fluid Phase Equilib.* **1988**, *41*, 257.
- Rhodes, J. M.; Bhethanabotla, V. R.; Campbell, S. W. *J. Chem. Eng. Data* **1997**, *42*, 731.
- Gupta, R. B.; Brinkley, R. L. *AIChE J.* **1998**, *44*, 207.
- Panagiotopoulos, A. Z. *Mol. Phys.* **1987**, *61*, 813–826.
- van Leeuwen, M. E.; Smit, B. *J. Phys. Chem.* **1995**, *99*, 1831.
- van Leeuwen, M. E. *Mol. Phys.* **1996**, *87*, 87.
- Chen, B.; Potoff, J. J.; Siepmann, J. I. *J. Phys. Chem. B* **2001**, *105*, 3093.
- Potoff, J. J.; Errington, J. R.; Panagiotopoulos, A. Z. *Mol. Phys.* **1999**, *97*, 1073.
- Nath, S. K.; Escobedo, F. A.; de Pablo, J. J. *J. Chem. Phys.* **1998**, *108*, 9905.
- Nath, S. K.; de Pablo, J. J. *Mol. Phys.* **2000**, *98*, 231.
- Nath, S. K.; Banaszak, B. J.; de Pablo, J. J. *J. Chem. Phys.* **2001**, *114*, 3612.
- Nath, S. K.; Banaszak, B. J.; dePablo, J. J. *Macromolecules* **2001**, *34*, 7841.
- Sum, A. K.; Biddy, M. J.; de Pablo, J. J.; Tupi, M. J. *J. Phys. Chem. B* **2003**, *107*, 14443.
- Nath, S. K. *J. Phys. Chem. B* **2003**, *107*, 9498.
- McGrother, S.; Nath, S. K.; Sum, A. K.; de Pablo, J. J. unpublished work.
- Nath, S. K.; Khare, R.; Meunier, M.; McGrother, S.; Sum, A.; de Pablo, J. J. AIChE Annual Meeting, Indianapolis, IN, 2002; Paper 399d.
- Rigby, D. *Fluid Phase Equilib.* **2003**, accepted for publication.
- Allen, M. P.; Tildesley, D. J. *Computer Simulation of Liquid*; Oxford University Press: New York, 1987.
- Frisch, M. J.; Trucks, G. W.; Schlegel, H. B.; Scuseria, G. E.; Robb, M. A.; Cheeseman, J. R.; Zakrzewski, V. G.; Montgomery, J. A.; Stratmann, R. E.; Burant, J. C.; Dapprich, S.; Millam, J. M.; Daniels, A. D.; Kudin, K. N.; Strain, M. C.; Farkas, O.; Tomasi, J.; Barone, V.; Cossi, M.; Cammi, R.; Mennucci, B.; Pomelli, C.; Adamo, C.; Clifford, S.; Ochterski, J.; Petersson, G. A.; Ayala, P. Y.; Cui, Q.; Morokuma, K.; Malick, D. K.; Rabuck, A. D.; Raghavachari, K.; Foresman, J. B.; Cioslowski, J.; Ortiz, J. V.; Stefanov, B. B.; Liu, G.; Liashenko, A.; Piskorz, P.; Komaromi, I.; Gomperts, R.; Martin, R. L.; Fox, D. J.; Keith, T.; Al-Laham, M. A.; Peng, C. Y.; Nanayakkara, A.; Gonzalez, C.; Challacombe, M.; Gill, P. M. W.; Johnson, B. G.; Chen, W.; Wong, M. W.; Andres, J. L.; Head-Gordon, M.; Replogle, E. S.; Pople, J. A. *Gaussian 98*, revision A.9; Gaussian, Inc.: Pittsburgh, PA, 1998.
- CRC Handbook of Chemistry and Physics*, 76th ed.; Lide, D. R., Ed.; CRC: Boca Raton, FL, 1995.
- Kiyohara, K.; Gubbins, K. E.; Panagiotopoulos, A. Z. *Mol. Phys.* **1998**, *94*, 803.
- Equilibria Module*, MS Modeling Version 2.2.1; Accelrys Inc.: San Diego, CA, 2003.
- Ding, H.-Q.; Karasawa, N.; Goddard, W. A., III. *J. Chem. Phys.* **1992**, *97*, 4309.
- Brooks, B. R.; Brucoleri, R. E.; Olafson, B. D.; States, D. J.; Swaminathan, S.; Karplus, M. *J. Comput. Chem.* **1983**, *4*, 187.
- Sun, H. *J. Phys. Chem. B* **1998**, *102*, 7338.
- Martin, M. G.; Siepmann, J. I. *J. Phys. Chem. B* **1998**, *102*, 2569.
- Nath, S. K.; Khare, R. *J. Chem. Phys.* **2001**, *115*, 10837.
- Chen et al. (ref 13) have used exponent values of 0.28 for ethanol and 0.29 for propanol, pentanol, and octanol. On the basis of this, we have used an exponent of 0.28 for ethanol and 0.29 for all other linear alcohols from propanol to octanol.
- Discover Module*, MS Modeling Version 3.0; Accelrys Inc.: San Diego, CA, 2003.
- NIST Chemistry WebBook*; NIST Standard Reference Database Number 69; Linstrom, P. J., Mallard, W. G., Eds.; National Institute of Standards and Technology: Gaithersburg, MD, March 2003; (<http://webbook.nist.gov>).